

TEMPERATURE INFLUENCE IN DEWATERING OPERATIONS IN A RISER

Angela O. Nieckele

Luis Fernando A. Azevedo

Arthur M. Braga

Departamento Engenharia Mecânica, PUC-Rio, 22453-900 Rio de Janeiro - RJ – BRASIL
nieckele@mec.puc-rio.br; lfaa@mec.puc-rio.br; abraga@mec.puc-rio.br

Abstract

Simulation of the dynamics of pig through non-isothermal flow in a riser is presented. The differential mass, linear momentum and energy equations were numerically solved by a finite difference numerical scheme, for compressible flow through pipelines. The fluid flow equations were combined with an equation representing a force balance on the pig. Pressure forces developed due to flow through by-pass holes in the pig, pig acceleration and pig/pipe contact forces were considered. A stick/slip model was developed to account for the distinct friction regimes that prevail depending on whether the pig is at rest or in motion. An adaptive grid technique was employed to account for the moving pig. A heat loss to the ambient plays a important hole in the temperature distribution. The temperature directly affects the fluid properties and as a consequence the pig dynamics. However, a significant effect is only felt for extreme pressure/temperature variations.

Keywords: Pipeline Pigging, Numerical Simulation, Compressible Non-Isothermal Flow

1. INTRODUCTION

Pigs are normally utilized in different stages of the pipeline life to perform operations such as, dewatering, cleaning, or internal inspection for damage or corrosion spots. In general terms, a pig is a solid cylindrical plug driven through the pipeline by the flowing fluid. Contact forces between the pig and the pipe wall are developed due to the oversize of the pig and should be overcome by the driving pressure provided by the flow.

The use of pigs has become a standard industry procedure. This expanding demand has driven manufacturers to produce a great variety of pig models. Yet, a difficulty often faced by the engineer when designing a pigging operation is the lack of reliable tools for the prediction of the many variables related to the motion of the pig through the pipeline. Most of the available knowledge is based on field experience. Hence, selecting the best pig, estimating its speed, required driving pressure and the amount of back and forward bypass of fluid, often involves some guesswork and, consequently, a high degree of uncertainty.

Figure 1 illustrates a typical type of pig, employed for cleaning operation. It is assembled from flat disk cups, usually made from polyurethane elastomer, attached to a cylindrical body. The cups can also have a conical shape. Polyurethane foam pigs, cast in cylindrical shapes, are also ordinarily used in cleaning operations. Fluid pumped upstream of the pig provides the necessary pressure difference to overcome the contact force at the

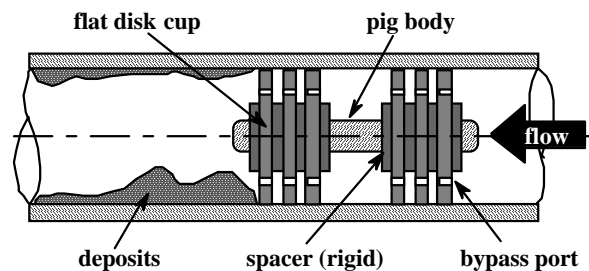


Figure 1. Schematic View of a Cleaning Pig.

wall, to remove the deposits and to accelerate the pig. In order to produce efficient cleaning and sealing, pigs have normally nominal diameters larger than the pipe diameter. Some pigs present passages in the cup or in the body to allow some fluid flow through the pig. Bypass is used to control the pig velocity and to avoid that deposits removed in a cleaning operation accumulate downstream of the pig, forcing it to stall.

A literature survey reveals very few papers dealing with the motion of pigs in pipelines. Most of the available work is based on field experience, being of limited scope. Haun (1986) and Burt & MacDonald (1997) treat the dynamics of simplified pigs in gas lines. General guidelines for the design of pigs are presented by Cordell (1986). Modeling of the pig-pipe contact forces is presented by Gomes (1994). Short (1994) conducted an experimental research program aimed at the understanding of the fundamental problems related to pipeline pigging. A simple model to predict the pig motion driven by incompressible fluids under steady state conditions was presented by Azevedo et al. (1995). Recently, Azevedo et al. (1997), analyzed the by-pass flow and contact forces in pigs. Santos et al. (1997), modeled the pig dynamics for pig-lift applications. Vianes Campo & Rachid (1997), studied the dynamics of pigs through pipelines using the method of characteristics.

At the present work the influence of the temperature distribution in the flow field and in pig dynamics is investigated. Since the pipeline can pass through different types of terrain, different ambient temperature and overall heat transfer coefficient can be specified along the pipeline. The temperature distribution affects directly the fluid properties and as a consequence the pig dynamics.

2. FLUID FLOW MODELING AND PIG DYNAMICS

The motion of a pig inside a pipe can be obtained by the solution of the fluid flow problem, coupled with a model to predict the pig motion. At the present work, the fluid flowing in the pipeline is considered to be Newtonian. Thus, the flow problem is governed by the conservation of mass, the linear momentum, and the energy equations.

It is assumed that the flow is one-dimensional, however, the centerline of the duct can be inclined with the horizontal at an angle α . Pipe deformation effects due to pressure variations along the fluid are considered. The mass conservation equation can be written as (Wylie and Streeter, 1978)

$$\frac{\partial p}{\partial t} + V \frac{\partial p}{\partial x} + \frac{\rho a^2}{\xi} \left[\frac{\partial V}{\partial x} + \frac{V}{A} \frac{\partial A}{\partial x} + \frac{\beta}{c_p} \left(\frac{\partial h}{\partial t} + V \frac{\partial h}{\partial x} \right) \right] = 0 \quad (1)$$

where V , p , h are the velocity, pressure and enthalpy, respectively. The fluid properties are: density ρ , speed of sound a , specific heat at constant pressure c_p , coefficient of thermal expansion β . A is the cross section area. ξ is given by $\xi = 1 + \rho a^2 2 C_D (D/D_{ref})$ where D and D_{ref} are the pipeline diameter and the reference diameter determined at atmospheric pressure p_{atm} . The pipe deformation due to pressure is accounted by the coefficient C_D , given by $C_D = (1 - \mu^2) D_{ref} / (2 e E)$, where e is the pipe wall thickness, E the Young's modulus of elasticity of the pipe material, and μ the Poisson's ratio.

The linear momentum equation can be written as

$$\frac{\partial V}{\partial t} + V \frac{\partial V}{\partial x} = - \frac{1}{\rho} \frac{\partial p}{\partial x} - \frac{f}{2} \frac{|V| V}{D} - g \sin \alpha \quad (2)$$

where g is gravity and f the hydrodynamic friction coefficient factor, which depends on the Reynolds number $Re = \rho |V| D / \mu_f$, where μ_f is the absolute viscosity. In the turbulent regime the friction factor is also a function of the relative pipe roughness ϵ/D . It can be approximated

by its fully developed expression. For a laminar regime, $Re < 2300$, it is specified as $f = 64/Re$. For the turbulent regime, $Re > 2300$, the friction factor is approximated by Miller's correlation (Fox and McDonald, 1995), $f = 0,25 \{ \log [(\epsilon/D)/3.7 + 5.74/Re^{0.9}] \}^{-2}$.

The energy conservation equation can be written as

$$\frac{\partial h}{\partial t} + V \frac{\partial h}{\partial x} = \frac{1}{\rho} \left[\frac{\partial p}{\partial t} + V \frac{\partial p}{\partial x} \right] + \frac{f}{2} \frac{V^2 |V|}{D} + \frac{1}{\rho A} \left[\frac{\partial}{\partial x} \left(\frac{k A}{c_p} \frac{\partial h}{\partial x} \right) \right] - \frac{4 U_G}{\rho c_p D} (h - h_\infty) \quad (3)$$

where k is the thermal conductivity and U_G is the global heat transfer coefficient between the fluid inside the pipe and the ambient, which is considered at a temperature T_∞ , and h_∞ is the corresponding ambient enthalpy.

The coupling of the pig motion with the fluid flow in the pipeline is obtained through a balance of forces acting on the pig (Azevedo et al., 1997), which can be written as

$$m \, dV_p / dt = (p_1 - p_2) A - m g \sin \alpha - F_{at}(V_p) \quad (4)$$

where, V_p is the pig velocity, m the pig mass, p_1 and p_2 the pressure on the upstream and downstream faces of the pig, α is the angle of the pipe axis with the horizontal.

The pressure drop across the pig is modeled as a localized pressure drop in order to take into account the possibility of the presence of bypass holes. Thus $p_1 - p_2 = K \rho V_h^2 / 2$, where K is the localized pressure drop coefficient and V_h is the fluid velocity at the bypass hole, measured relatively to the moving pig. Assuming the flow to be locally incompressible, a mass conservation equation can be written for a control volume moving with the pig. Thus, $Q_h = Q - V_p A$, where Q_h is the volume flow rate through the bypass hole, Q is the flow rate through the pipe upstream of the pig, V_p is the pig velocity and A the pipe area. The pressure drop across the pig, can then be written as (Azevedo et al., 1995)

$$p_1 - p_2 = (\rho K / 2) (A / A_h)^2 (Q / A - V_p)^2 \quad (5)$$

where A_h is the hole cross sectional area. Note that Q/A is the average fluid velocity approaching the pig.

The term $F_{at}(V_p)$ in equation 3 represents the contact force between the pig and the pipe wall. When the pig is not in motion, the contact force varies from zero to the maximum static force, F_{stat} in order to balance the pressure force due to the fluid flow. In case the pressure gradient is negative, this maximum force is F_{stat}^{neg} . If the pressure gradient is positive, the maximum force is F_{stat}^{pos} . These two values of forces are not necessarily equal since the pig may resist differently to being pushed forward or backward.

Once the pig is set in motion by the flow, the contact force assumes the constant value, F_{dyn} , representing the dynamic friction force that is generally different from the static force. As in the previous situation, two different values for the dynamic contact force are allowed, F_{dyn}^{neg} and F_{dyn}^{pos} , depending on the direction of the pig motion.

The contact force depends on x_p , the pig axial coordinate, indicating that it can vary along the pipe length. The values assumed by the contact force can be summarized as follows,

$$F_{at}(V_p) = \begin{cases} -F_{din}^{neg}(x_p) & \text{if } V_p < 0 \\ F(x_p) & \text{if } V_p = 0 \text{ where } -F_{stat}^{neg}(x_p) \leq F(x_p) \leq F_{stat}^{pos}(x_p) \\ F_{din}^{pos}(x_p) & \text{if } V_p > 0 \end{cases} \quad (6)$$

2.1 Fluid properties

The gas is considered to behave as an ideal gas, therefore the density ρ , the isothermal speed of sound a , the isentropic speed of sound c and thermal expansion coefficient β are obtained by

$$\rho = p / a^2 \quad ; \quad a^2 = R_{\text{gas}} T \quad ; \quad c = \sqrt{\gamma R_{\text{gas}} T} \quad ; \quad \beta = 1/T \quad (7)$$

where R_{gas} is the gas constant and $\gamma = c_p/c_v$ is the specific heat ratio, where c_p and c_v are the specific heat at constant pressure and constant volume, respectively.

Constant speed of sound a , and thermal expansion coefficient β are assumed for liquids, while the density is obtained by

$$\rho = \rho_{\text{ref}} [1 - \beta(T - T_{\text{ref}})] + (p - p_{\text{ref}}) / a^2 \quad (8)$$

where ρ_{ref} is the reference density evaluated the reference pressure p_{ref} and reference temperature T_{ref} .

For both liquids and gases, the fluid absolute viscosity can vary linearly with pressure and temperature, according to

$$\mu_f = \mu_{\text{ref}} + c_{\mu T} (T - T_{\text{ref}}) + c_{\mu p} (p - p_{\text{ref}}) \quad (9)$$

while the specific heat at constant pressure c_p , specific heat ratio γ , and thermal conductivity k are considered constant.

3. NUMERICAL METHOD

To better account for the motion of the pig in the pipeline the governing equations were re-written in terms of a coordinate system that stretches and contracts in the pipe, depending of the pig position.

The set formed by equations (1) to (6), together with the appropriate boundary and initial conditions, require a numerical method to obtain the desired time-dependent pressure and velocity fields. These equations were discretized by a finite difference method. A staggered mesh distribution, was selected to avoid unrealistic oscillatory solutions, as recommended by Patankar, 1980. The equations were integrated in time, using a totally implicit method. The space derivatives were approximated by the central difference method around the mesh point. The resulting coefficient matrix is hepta-diagonal, and can be easily solved by a direct hepta-diagonal algorithm.

The total number of grid points inside the pipe, was maintained constant in the numerical calculations of the flow field upstream and downstream of the pig, and of the pig dynamics itself. However, as the pig moves along the pipe, an adaptive mesh technique was employed to rearrange the node distribution. The number of grid points upstream and downstream of the pig was made proportional to the length of the pipe at each side of the pig. Further, the mesh was concentrated near the pig to better resolve the steeper gradients of the flow properties in this region.

4. ANALYSIS

At the present work, the problem investigated, consists on a dewatering operation in a riser configuration typically encountered in sub-sea oil production lines is studied. The riser is initially filled with water and nitrogen is injected to displace the water out of the pipe. A sealing pig separates the two fluids.

The reference fluid properties were $P_{ref} = 1 \text{ atm}$; $T_{ref} = 25 \text{ C}$. The properties were: (i) Nitrogen: $R_{gas} = 296.9 \text{ J/(kg K)}$; $\gamma = 1.4$; $\mu_{ref} = 1.88 \cdot 10^{-5} \text{ N s/m}^2$; $c_{\mu T} = 2.255 \cdot 10^{-8} \text{ N s/(m}^2 \text{ K)}$; $c_{\mu p} = 0$; $c_p = 1.042 \cdot 10^3 \text{ J/(kg K)}$; $k = 2.2 \cdot 10^{-2} \text{ W/(m K)}$. (ii) water: $\rho_{ref} = 1000 \text{ kg/m}^3$, $a = 1200 \text{ m/s}$; $\mu_{ref} = 7.58 \cdot 10^{-4} \text{ N s/m}^2$, $c_{\mu T} = -4.5 \cdot 10^{-5} \text{ N s/(m}^2 \text{ K)}$; $c_{\mu p} = 0$, $c_p = 4.18 \cdot 10^3 \text{ J/(kg K)}$; $k = 0,6 \text{ W/(m K)}$.

Figure 2 shows the simplified riser geometry adopted. Gas is pumped at the inlet with the objective of displacing the liquid initially filling the pipe. The inlet and outlet are at sea level, thus the ambient temperature are 25 C, and the overall heat transfer coefficient is $50 \text{ W/(m}^2 \text{ K)}$. From point 1 to 7, the pipeline is under water, and the global heat transfer coefficient is $500 \text{ W/(m}^2 \text{ K)}$. The ambient temperature drops 1 C every 30 m, reaching the value of 4 C in the bottom (stations 3 to 5). As will be seen in the results to be presented, the change in elevation of the riser is responsible for an interesting pig dynamic behavior.

Table 1. Riser geometric parameters

Position	x (m)	y(m)	Position	x(m)	y(m)
Inlet	0	0	Point 5:	250	-600
Point 1	50	0	Point 6:	250	-300
Point 2	50	-300	Point 7:	250	0
Point 3	50	-600	Outlet:	300	0
Point 4	150	-600			

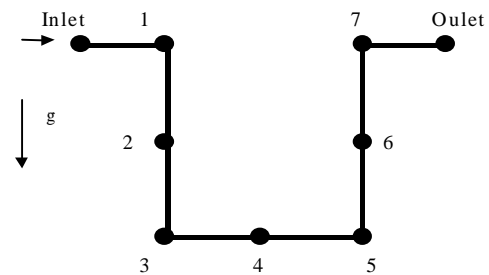


Figure 2. Riser geometry

The total length of the riser is equal to 1500 m. The results to be presented are referenced to the seven stations marked in the figure. In the simulations, the following pipe characteristics were used: diameter: $D = 10 \text{ in}$, wall thickness: $e = 6 \text{ mm}$, relative roughness: $\epsilon/D = 1.8 \cdot 10^{-4}$, Young's modulus of elasticity: $E = 2 \cdot 10^5 \text{ MPa}$, Poisson's coefficient: $\mu = 0.3$.

A 3-kg pig was used in the dewatering process. The positive and negative static force values were taken as equal to 4982 N, the same value adopted for the positive and negative dynamic forces.

Initially the fluid was at rest, with the same temperature distribution as the ambient and with a hydrostatic pressure distribution was prescribed. The outlet pressure was kept constant and equal to 10 atm. The inlet gas mass flow rate varied linearly with time during 10 seconds, reaching the value of 3 kg/s, being kept constant after that. Initially the pig had zero velocity, and was positioned at the pipe entrance section.

The time variation of pressure is shown in Figure 3, while the gas and liquid mass flow rate are shown in Figure 4 and 5. The temperature distribution can be seen in Figure 6. The pig dynamics are shown in Figures 7 and 8, for the present non isothermal situation, and for an isothermal one, with the fluid kept at 25 C. Reference to Figure 8 can help identify the pig position each time. The isothermal problem has been investigated by Azevedo et al, 1998. The pressure and mass flow rate distribution for the isothermal and non isothermal situations is almost coincident and only one situation is represented.

It can be seen in Figure 3 that, while the outlet pressure is kept constant, the inlet pressure increases with time, until the pig reaches point 3 at the base of the riser. This behavior can be justified by noting that, as the pig moves downwards through the riser, the hydrostatic pressure to be overcome increases. As the pig moves from station 3 to 5, the inlet pressure is almost constant, because the hydrostatic column is also

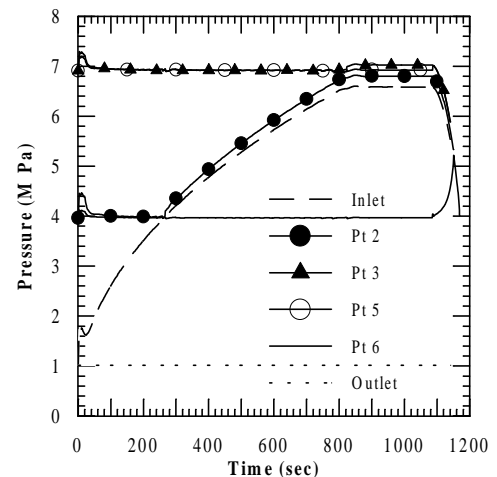


Figure 3. Pressure

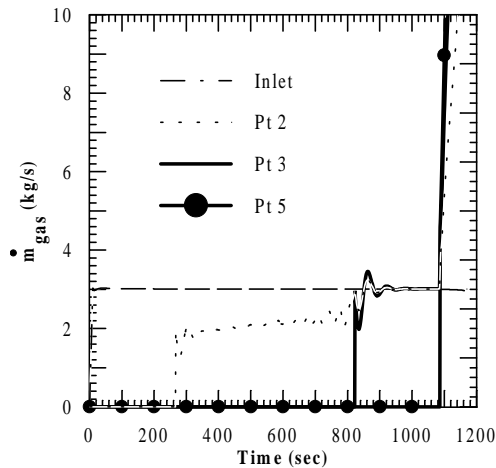


Figure 4. Gas mass flow rate

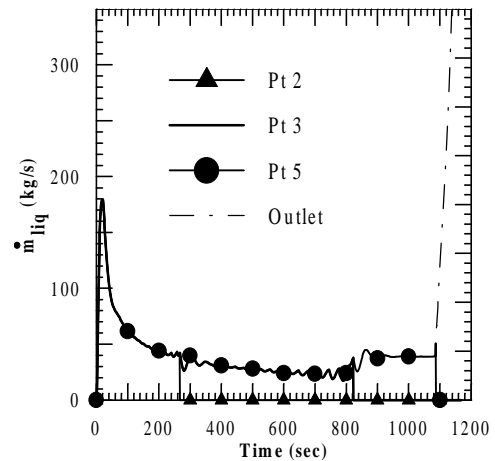


Figure 5. Liquid mass flow rate

constant. After that, the inlet pressure decays sharply, as the pig starts its ascending motion, decreasing the hydrostatic column to be displaced. The pig velocity increases sharply. In order to maintain these high flow rate levels, the fluid pressure also increases sharply until the pig reaches station 6, when, as with all other points, the pressure decreases.

The time variation of the gas mass flow rate is shown in Figure 4, for four positions in the riser. The inlet mass flow rate attains a constant value very rapidly. At station 2, the gas mass flow rate is zero until the pig reaches that position. Then, it gradually increases, reaching a constant value similar to the inlet mass flow rate, while the pig moves from 3 to 5. A similar behavior is also observed for station 3. Note that when the pig reaches point 5 (time approximately equal to 1100 s) and starts its ascending motion, the pig velocity increases sharply because of the smaller water column to be overcome. Consequently, the mass flow rate at the stations located upstream of the pig also increase sharply.

The time variation of the liquid mass flow rate through the riser is shown in Figure 5. With the exception of the exit section, all other stations present a similar mass flow variation, but shifted in time. Initially, the mass flow rate increases as the pig is accelerated and start displacing the water. As the pig passes through a particular station, that position is exposed to the gas and the liquid mass flow rate immediately drops to zero. This happens for point 2 at 260 seconds, for point 3 at 820 s, and for point 5 at 1100 s. At the exit station, the liquid mass flow rate follows, initially, the same behavior as the other stations. However, as the pig accelerates in the vertical section of the riser, a sharp increase in the mass flow rate is produced. In practical applications the liquid receiving facilities at the platform would have to be designed to handle these very high flow rates produced by the accelerated, upward-moving pig.

Figure 6 illustrates the time variation of temperature at the different stations. At the inlet, nitrogen is continuously injected at 25 C. After just a few seconds, the pig has passed by station 1. From the inlet to station 1, the ambient temperature is constant and equal to the ambient. The temperature shows an increase due to the pressure increase, followed by slow decrease until the pig reaches the bottom of the riser. While the pig moves from station 3 to 5, both pressure and temperature are approximately constant. At station 2, the water is initially at 15 C. Until the pig reaches this station (≈ 200 s), the water pressure is approximately constant, and its temperature increases with the incoming warmer water. After the pig passes by station 2, the hydrostatic pressure that it has to overcome is higher and the pressure increases at its back. A sharp drop in the temperature is observed after the passage of the pig, when the fluid at the station changes from water to nitrogen, since the latter has a much lower specific heat. The temperature is maintained constant until the pig passes by station 5 when a sharp drop in temperature and pressure are observed due to the substantial pig velocity increase. A similar temperature behavior is observed at stations (3), (4) and (5). At station (6), colder water is

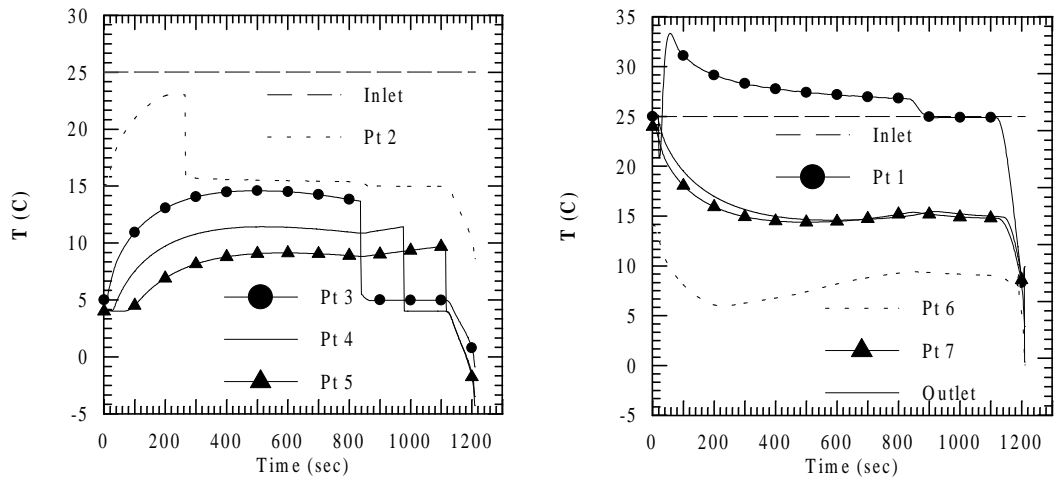


Figure 6. Temperature variation with time

pushed by the pig, resulting in a decrease of temperature. However, since the temperature increases in the downstream stations, the heat transfer from the ambient increases the water temperature at this station. Once again, there is a sharp drop on pressure and temperature when the pig reaches station 5 and its velocity increases substantially. A similar behavior is observed at station (7), which presents the same temperature distribution as the outlet section.

Figure 7 presents the pig velocity as a function of its position along the riser. The results presented show that the pig is initially accelerated sharply as it goes from the inlet to station 1, as a consequence of the small hydrostatic pressure ahead of the pig. As the pig moves down along the left leg of the riser, the velocity decreases as the hydrostatic column increases. The pig velocity is approximately constant along the initial portion of the horizontal part of the riser. However, as the pig approaches the end of the horizontal leg (station 5), it is accelerated due to the decreasing resistance offered by the liquid flow that is being progressively driven out of the pipe. After the pig passes station 5 and begins to ascend in the riser, its velocity continues to increase due to the decreasing hydrostatic pressure. The velocity levels attained by the pig in the simulations are similar to those verified in field operations. These high velocity levels should be avoided at the risk of causing damage to the platform facilities. Note that, although the temperature variation is larger in the water than for the nitrogen, its influence in the water flow is quite small and it is slightly higher in the nitrogen flow. Its effect is only felt, when high velocities and strong pressure gradients are encountered.

Figure 8 presents the pig position along the riser as a function of time. The two horizontal lines plotted in the figure represent the position of stations 3 and 5, and were included to

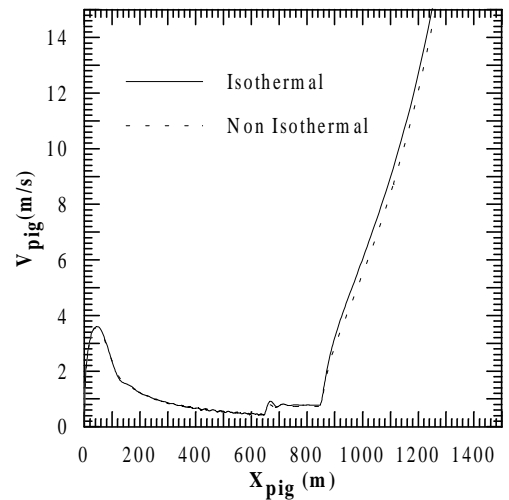


Figure 7. Pig velocity versus pig position.

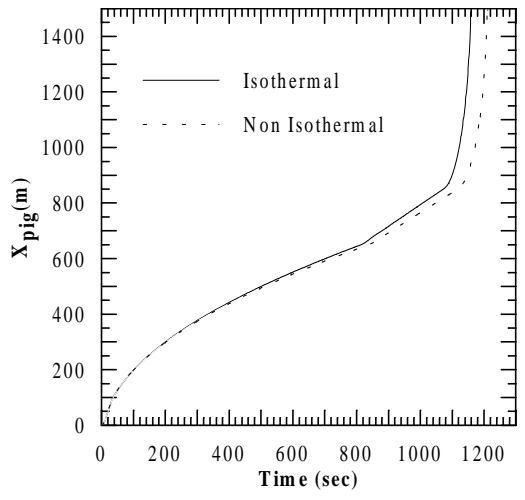


Figure 8. Pig position with time.

facilitate the analysis of the pig motion. The temperature distribution has a very small effect on the flow field and consequently in the pig dynamics. Due to the temperature gradient there is a slightly delay of the pig arrival at station 5, when it then shoots off.

5. CONCLUSION

The present paper presented a simulation of the fluid flow/heat transfer and pig dynamics of a dewatering operation in a riser. The basic equations governing conservation of mass, linear momentum and energy were numerically solved. Although the heat loss to the ambient and heat transfer within the pipeline is significant, a very small effect in the fluid flow was observed. In both isothermal and non-isothermal cases simulated, the pig attained very high velocities at the end of the operation. These are potentially dangerous situations that should be avoided by proper pig design.

6. ACKNOWLEDGEMENTS

The authors gratefully acknowledge the support awarded to this research by the following companies: Petrobras, Ancap, Norsk Hydro, Statoil, Saga Petroleum, Pipetronix, Halliburton, Exxon P. R., Texaco, and Ecopetrol.

7. REFERENCES

- Azevedo, L.F.A. Braga, A.M.B., Nieckele, A.O., Naccache, M.F and Gomes, M.G.F., 1995, "Simple hydrodynamic models for the prediction of pig motion in pipelines", Proceedings of the Pipeline Pigging Conference, Houston, USA.
- Azevedo, L.F.A., Braga, A.M.B. and Gomes M.G.F.M., 1997, "Experimental Validation of Analytical Numerical Models for By-pass Flow and Contact Forces in Pig Cups", The Pipeline Pigging Conference, Houston, USA.
- Azevedo, L.F.A. Braga, A.M.B., Nieckele, A.O., 1998, "Simulation Of Fluid Flow And Pig Dynamics In Dewatering Operations In Pipelines", 1998 ENCIT, Encontro Nacional De Ciências Térmicas, Rio De Janeiro, RJ, Brasil, V. 2, pp.1025-1030.
- Burt, E. G.C. & MacDonald, R., 1997, "Pig Signaling, Location and Tracking", The Pipeline Pigging Conference, Houston, USA.
- Cordell, J.L., 1986, "Design of Pigs for Subsea Systems", Proceedings of the 1986 Conference on Subsea pigging, Haugesund, Norway, Pipes & Pipelines International.
- Fox, R. W. and McDonald, A. T., "Introdução à Mecânica dos Fluidos", Ed. Guanabara, 1995.
- Gomes, M.G.F.M., "Finite Element Analysis of Pig Cups for Pipeline Cleaning", 1994, Master Thesis, Department of Mechanical Engineering, Federal University of Rio de Janeiro (in Portuguese).
- Haun, R., 1986, "Analysis and Modeling of Pipeline Dewatering and Startup, Part 1", Pipeline Industry, February, pp.37-41.
- Patankar, S.V., 1980, "Numerical Heat Transfer and Fluid Flow"; Hemisphere Publishing Corporation, New York.
- Santos, O. G., Alhanati, J.S. & Bordalo, S. N., 1997, "Modeling and Performance of Pig-Lift", XIV COBEM, SP, Brasil, COB260, CD-ROM.
- Short, G.C., 1994, "The Pigging Technology Project: The First Three Years", Pipes & Pipelines International, Vol. 39-4, pp.23-27.
- Vianes Campo, E. & Rachid, F.B., 1997, "Modeling of Pig Motion Under Transient Fluid Flow", XIV COBEM, SP, Brasil.
- Wylie & Streeter, 1978, "Compressible Flow in Pipes", McGraw Hill.